Contemporary Engineering Sciences, Vol. 7, 2014, no. 12, 589 - 602
HIKARI Ltd, www.m-hikari.com
http://dx.doi.org/10.12988/ces.2014.4437

The Pre-mixer Model of New Intake Manifold System Application for Multi-fuel Spark Ignition Engine by Numerical Investigation and Comparison

Thanakom Soontornchainacksaeng

Energy Management Systems and Monitoring & Verification Control, Research & Development Center Science and Technology Research Institute (STRI)
Department of Mechanical and Aerospace Engineering
King Mongkut's University of Technology North Bangkok
1518 Pracharat 1 Road,Wongsawang, Bangsue, Bangkok 10800, Thailand

Paramust Juntarakod

Department of Mechanical and Aerospace Engineering
King Mongkut's University of Technology North Bangkok
1518 Pracharat 1 Road,Wongsawang, Bangsue, Bangkok 10800, thailand

Abstract

This paper is to study about the development of variable intake manifold for spark ignition engine. Variable intake manifold by numerical is one of the methods in optimizing the performance of an engine when changing or mixing fuel. It has been found that the geometric of new multi fuel intake system configurations of spark ignition engine plays a vital role in engine performance. The main aims of the paper are to assess the comprised thermal efficiency and numerical engine performances for the multi fuel small spark ignition engine of modified intake system unit. This engine type is unique, entirely conceived by the author and has not previously been reported in the open literatures. It is called the pre mixer of multi fuel and air. It was compared with the old intake manifold system of fuel injectors [8] and carburetor [10]. It makes this system can adjust the fuel mixture, or a variety of gasoline with ethanol, that aimed at engine improvements through thermodynamic engine indicated power (kW) with the indicated mean effective pressure (IMEP) and thermal efficiency (%) with specific fuel consumption (SEC, g/kW-hr) gains. The routine was written using MATLAB-based procedure for determining at different operating condition such as engine speed, equivalence ratio and compression ratio that describe the engine performance. The effect of equivalence ratio is affecting the system changes significantly of pre-mixer and carburetor with fuel injector in the thermal efficiency about 5-50%. The effect of compression ratio is affecting the system changes significantly of pre-mixer with carburetor and fuel injector for the thermal efficiency and SFC.

Keywords: Air-fuel models, thermodynamic models, spark ignition engines, Alternative Fuels, Carburetor and Fuel injection model

1 Introduction

In this section, the pre-mixer model (Air-fuel gas mixing) of small spark ignition engine was developed for gas pre-mixer design and analysis. In an important literature review for applied, as following the ejector of refrigerant system from Yapici and Wang [2], as following of refrigerant system ejector model from Chaqing [3], he wrote the rewrite equation (single phase area-constant, pressure-constant). But all model be applied to the pre-mixer between fuel gas injected (primary nozzle, $M_{p1} > 1$) and air inducted by the old intake system (secondary, $M_{s1} < 1$) as the condition of mixing chamber constant pressure. For most of the existing models, there is one way to determine the static pressures at the mixing chamber entrance (P_{p1}, P_{s1} and P_1), arbitrarily given. Where P_1 is represented by the product of two parameters, $\mu = P_1 / P_{s0}$ and $\tau = P_{s0} / P_{m2}$, which relate the boundary conditions to pre-mixer performance. The parameter τ is a parameter given as a downstream boundary condition, assumption are,

The control volume selected to analyze the flow in the mixing chamber is shown in the left hand section of Fig 1. In the analysis, the following assumptions were made,

1) The inner wall of the pre-mixer is adiabatic, friction loss is negligible.
2) The flow streams are uniform 1-D and in steady state.
3) Gases are in stagnation at the primary inlet and suction port.
4) The secondary flow is the two cases as subsonic and supersonic.
5) The primary stream and secondary stream have the same static pressure at the entrance of the mixing chamber, $P_{p1} = P_{s1} = P_1$.
6) The mixed flow is subsonic.
7) Both primary stream (Flash air) and secondary stream (Hydrocarbon gases fuel) can be considered as perfect gases with constant specific heat ratio γ.

$$m_t = m_{p\,(\mathrm{Air})} + m_{s\,(\mathrm{fuel\ g}}$$

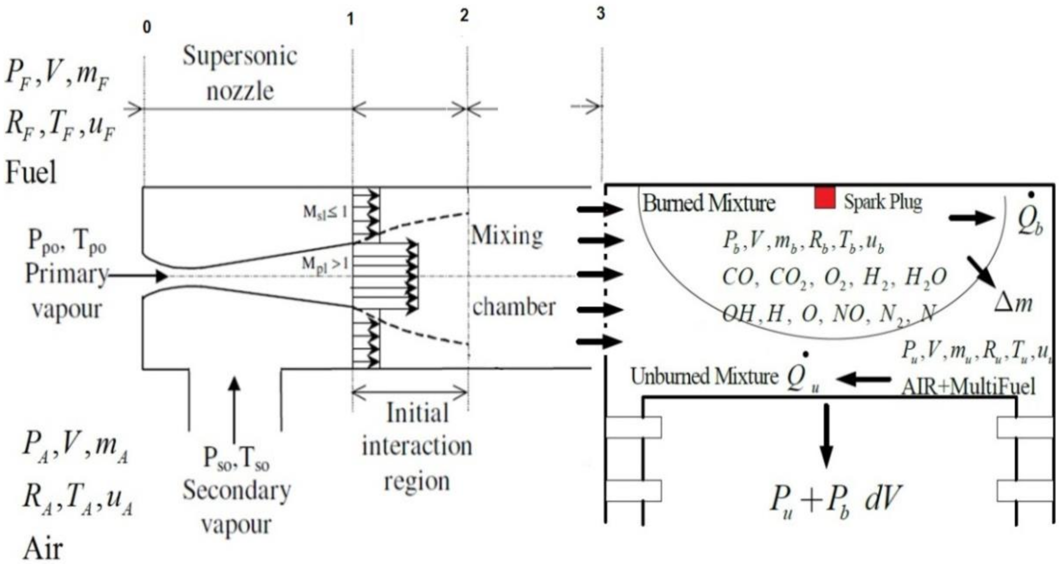

Figure 1 : Schematic of the pre-mixer model

2 Numerical Mixing Chamber of the Pre-Mixer

2.1 A schematic of the pre-mixer chamber

A schematic of the pre-mixer chamber is illustrated in Fig. 2 (point 2-3 Fig. 1). More in detail, the boundary layer of fuel and air is represented as a spherical surface of infinitesimal thickness, truncated by the mixing walls, propagating into the pre-mixer chamber. This surface subdivides the in cylinder charge into three zones: a first one, containing air gases behind; and a second one, made up of fresh fuel (this study assumed to be gas phase), a third one, containing mixing gases (mixture, subscription m), fills the volume beyond the layer. For the sake of simplicity, it is assumed that no exchange occurs between the three zones. As far as the in chamber charge is concerned, it is assumed that both air-fuel zones and mixture are mixtures of ideal gases, with different composition: unburned mixture consisting only of fuel and air (modeled as 21% O_2 and 79% N_2), and mixture gases composition computed according to a chemical equilibrium algorithm, described in next section, a total of eleven components is considered. The subdivision into three zones implies the definition of two different temperatures, each one assumed constant within air-fuel zone and mixture zone; conversely, pressure is the same throughout the mixing chamber as fooling the assumed next section. Finally, blow-by flow to crevices is neglected. From the first principle of thermodynamics or energy conservation, the following differential equations can be obtained Equation 8 to 11, see Paramust, [4 and 11].

$$\dot{T}_A = \left(\frac{\dot{m}_A \ h_F - u_A \ + \dot{Q}_A - P_A \dot{V} - V \left(\frac{\partial \ln v_A}{\partial \ln T_A} + \frac{\partial \ln v_A}{\partial \ln P_A} \right) \dot{P}_A}{\left(m_A c_{PA} - m_A R_A \frac{\partial \ln v_A}{\partial \ln T_A} \right)} \right) \tag{1}$$

$$\dot{T}_F = \left(\frac{ \dfrac{\dot{Q}_F}{m_F R_F} + T_F \dfrac{\dot{P}_F}{P_F} - v_F \left(\dfrac{\partial \ln v_F}{\partial \ln T_F} + \dfrac{\partial \ln v_F}{\partial \ln P_F} \right) \dfrac{\dot{P}_F}{R_F} }{ 1 + \left(\dfrac{c_{PF}}{R_F} - \dfrac{\partial \ln v_F}{\partial \ln T_F} \right) } \right) \tag{2}$$

$$\dot{m}_{A,-F} = \left(\frac{ \dot{Q}_A - P_A \dot{V} \left(1 + \left(\dfrac{c_{PA}}{R_A} - \dfrac{\partial \ln v_A}{\partial \ln T_A} \right) \right) - PV \left(\left(\dfrac{c_{PA}}{R_A} - \dfrac{\partial \ln v_A}{\partial \ln T_A} \right) + \left(\dfrac{\partial \ln v_A}{\partial \ln T_A} + \dfrac{\partial \ln v_A}{\partial \ln P_A} \right) \right) \left(1 + \dfrac{\dot{V}}{V} - \dfrac{\dot{T}_F}{T_F} \right) }{ \left(u_A - u_F \;\; - R_F T_F - \left(c_{PA} T_A - P v_A \dfrac{\partial \ln v_A}{\partial \ln T_A} \right) + P v_F \left(\left(\dfrac{c_{PA}}{R_A} - \dfrac{\partial \ln v_A}{\partial \ln T_A} \right) + \left(\dfrac{\partial \ln v_A}{\partial \ln T_A} + \dfrac{\partial \ln v_A}{\partial \ln P_A} \right) \right) \right) } \right) \tag{3}$$

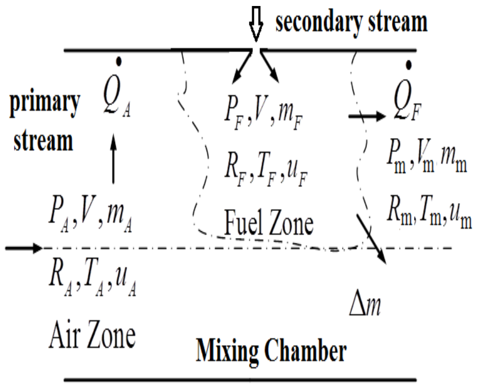

Figure 2 : Schematic of the mixing chamber (position of 1 to 2 from Fig. 1)

2.2 Two phase mixing flow intake system properties by difference Density

The T_{s1}/T_{p1} and T_{m2}/T_{p1} can be obtained by using the isentropic relationship between temperature and pressure,

$$\frac{T_{s1}}{T_{p1}} = \frac{T_{s0}}{T_{p0}} \left(\frac{P_{p0}}{P_1} \right)^{\frac{\gamma_p - 1}{\gamma_p}} \left(\frac{P_{s0}}{P_1} \right)^{-\frac{\gamma_s - 1}{\gamma_s}} \tag{7}$$

$$\frac{T_{m2}}{T_{p1}} = \frac{T_{m0}}{T_{p0}} \left(\frac{P_{p0}}{P_1} \right)^{\frac{\gamma_p - 1}{\gamma_p}} \left(\frac{P_{m0}}{P_1} \right)^{-\frac{\gamma_m - 1}{\gamma_m}} \tag{8}$$

$$\gamma_m = \frac{ \dfrac{\gamma_p}{\gamma_p - 1} + \dfrac{\gamma_s}{\gamma_s - 1} \dfrac{R_s}{R_p} \omega }{ \dfrac{1}{\gamma_p - 1} + \dfrac{1}{\gamma_s - 1} \dfrac{R_s}{R_p} \omega } \tag{9}$$

$$\frac{T_{m0}}{T_{p0}} = \frac{ \dfrac{\gamma_p}{\gamma_p - 1} + \dfrac{\gamma_s}{\gamma_s - 1} \dfrac{R_s}{R_p} \dfrac{T_{s0}}{T_{p0}} \omega }{ \dfrac{1}{\gamma_p - 1} + \dfrac{1}{\gamma_s - 1} \dfrac{R_s}{R_p} \omega } \tag{10}$$

The P_{m0}/P_{p0} can be obtained by using the isentropic function as,

$$\frac{P_{m0}}{P_1}=\left(1+\frac{\gamma_m-1}{2}M_{m2}^2\right)^{\frac{\gamma_m}{\gamma_m-1}} \tag{11}$$

If the velocity is supersonic after constant-pressure mixing, i.e., $M_{m2}>1.0$, a normal shock wave will occur between section 2 and section 3. Assuming the mixed flow after the shock undergoes an isentropic process, it has a uniform pressure T_{m3} in the constant area section. The follow parameters after the shock wave can be calculated by the following gas dynamic relationships.

$$\frac{P_{m3}}{P_{m2}}=\frac{2\gamma_m}{\gamma_m+1}M_{m2}^2-\frac{\gamma_m-1}{\gamma_m+1} \tag{12}$$

$$\frac{T_{m3}}{T_{m2}}=\left(\frac{\gamma_m+1}{\gamma_m+1}\right)^2\left(\frac{2\gamma_m}{\gamma_m+1}M_{m2}^2-1\right)\left[\frac{2}{(\gamma_m+1)M_{m2}^2}+1\right] \tag{13}$$

$$M_{m3}^2=\frac{M_{m2}^2+\dfrac{2}{\gamma_m+1}}{\dfrac{2\gamma_m}{(\gamma_m+1)}M_{m2}^2+1} \tag{14}$$

3 Engine Model of Spark Ignition Engine

3.1 The Mathematical model of engine

In the combustion stroke, we consider the temperature in the term of burned mixture (T_b) and unburned (T_u) as separate open systems [5, 6, 7, 8 and 9].

$$\frac{dP}{d\theta},\frac{dT_b}{d\theta},\frac{dT_u}{d\theta}=f_1(L,P,T_b,T_u) \tag{15}$$

Modified algorithm from Ferguson [8] as following the arbitrary heat release conditions and solving the above equations with appropriate input data enable determination of the indicated work, enthalpy and heat loss throughout the system. Those can be expressed as a function of pressure and indicated work.

$$\frac{dP}{d\theta}=\frac{A+B+C}{D+E} \tag{16}$$

$$\frac{dW}{d\theta}=P\frac{dV}{d\theta} \tag{17}$$

$$A=\frac{1}{m}\left(\frac{dV}{d\theta}+\frac{VC}{\mathrm{v}}\right) \tag{18}$$

$$B=h\frac{\left(\frac{dV}{d\theta}+\frac{VC}{\mathrm{v}}\right)}{\mathrm{v}m}\left(\frac{v_b}{\mathrm{c_{Pb}}}\frac{\partial\ln v_b}{\partial\ln T_b}x^{1/2}\frac{T_b-T_W}{T_b}+\frac{v_u}{\mathrm{c_{Pu}}}\frac{\partial\ln v_u}{\partial\ln T_u}\ 1-x^{1/2}\ \frac{T_b-T_W}{T_b}\right) \tag{19}$$

$$C=-\ v_b-v_u\ \frac{dx}{d\theta}-v_b\frac{\partial\ln v_b}{\partial\ln T_b}\frac{h_u-h_b}{\mathrm{c_{Pb}}T_b}\left[\frac{dx}{d\theta}-\frac{(x-x^2)C}{\mathrm{v}}\right] \tag{20}$$

$$D = x\left[\frac{v_b^2}{c_{Pb}T_b}\left(\frac{\partial \ln v_b}{\partial \ln T_b}\right)^2 + \frac{v_b}{P}\frac{\partial \ln v_b}{\partial \ln P}\right] \tag{21}$$

$$E = 1 - x\left[\frac{v_u^2}{c_{Pu}T_u}\left(\frac{\partial \ln v_u}{\partial \ln T_u}\right)^2 + \frac{v_u}{P}\frac{\partial \ln v_u}{\partial \ln P}\right] \tag{22}$$

The derivative form of the slider-crank model is given as a non-dimensional relationship is described as following equation Ferguson [8].

3.2 Multi fuel Combustion Model at Combustion Stroke

The basis of the equilibrium combustion products with fuel mixture model $C_\alpha H_\beta O_\gamma N_\delta$ is a solution to the atom balance equations from the chemical reaction equation of fuel and air forming and The subscript 1 and 2 represent the one of the fuel (Gasoline) and the fuel in the second (Ethanol) respectively. This mixture equation is given in Eq. (52) for the condition of equivalence ratio ϕ, where ν_1 through ν_{11} are mole fractions of the product species, ε is the molar fuel-air ratio required to react with one mole of air. This process based on the work of modified Paramust [5] as given below,

$$\begin{array}{lcl} \varepsilon\phi(1-\chi_1)C_{\alpha1}H_{\beta1}O_{\gamma1}N_{\delta1} + & & \nu_1 CO_2 + \nu_2 H_2O + \nu_3 N_2 \\ \varepsilon\phi(\chi_1)\ \chi_2 C_{\alpha2}H_{\beta2}O_{\gamma2}N_{\delta2} & \rightarrow & +\nu_4 O_2 + \nu_5 CO + \nu_6 H_2 \\ & & +\nu_7 H + \nu_8 O \\ +0.21O_2 + 0.79N_2 & & +\nu_9 OH \nu_{10} NO + v_{11} N \end{array} \tag{15}$$

Where χ_1 is the molar ratio of multi-fuel having the condition ($0 < \chi_1 < 1$). χ_2 is the fuel in the second which having the condition($\chi_1 + \chi_2 = 1$). There is the conservation of 4 atoms, C,H,O and N from mixture equation, so atom balancing can be written,

$$\text{C} \quad \varepsilon\phi(1-\chi_1)\alpha1 + \varepsilon\phi\chi_1\chi_2\alpha2 = (y_1 + y_5)\,N \tag{16}$$

$$\text{H} \quad \varepsilon\phi(1-\chi_1)\beta1 + \varepsilon\phi\chi_1\chi_2\beta2 = (2y_2 + 2y_6 + y_7 + y_9)N \tag{17}$$

$$\text{O} \quad \varepsilon\phi(1-\chi_1)\gamma1 + \varepsilon\phi\chi_1\chi_2\gamma2 + 0.42 = (2y_1 + y_2 + 2y_4 + y_5 + y_8 + y_9 + y_{10})N \tag{18}$$

$$\text{N} \quad \varepsilon\phi(1-\chi_1)\delta1 + \varepsilon\phi\chi_1\chi_2\delta2 + 1.58 = (2y_3 + y_{10} + y_{11})N \tag{19}$$

Therefore in order to solve for these 11 unknowns other 7 more equations are needed this may be derived from the consideration of equilibrium among products. The method for solved all equation see [5, 6 and 7].

3.3 Engine Performance parameters

A study of gases as models of internal combustion engines is useful for qualitatively illustrating some of the important parameters influencing engine performances, that is, the work output w_{CV} from fuel-air cycle. In theoretical of control volume, the combustor performances can be calculated by meaning of the indicated values which the following definitions are done by the gas. That are, Thermal Efficiency (%)

$$\eta = \int_{-360}^{360} \frac{dW}{d\theta} \left(\frac{[1+\phi F_s (1-f)]}{\phi F_s a_0 (1-f)} \right) \tag{20}$$

The indicated mean effective pressure, (IMEP)

$$\text{IMEP} = \int_{-360}^{360} \frac{dW}{d\theta} \frac{[1+\phi F_s (1-f)]}{V} \tag{21}$$

The indicated power (kW)

$$power = \int_{-360}^{360} \frac{dW}{d\theta} d\theta \tag{22}$$

The specific fuel consumption (SEC, g/kW-hr)

$$SFC = \frac{\dot{m}_f (LHV)}{power} \tag{23}$$

4 Results and Discussions

4.1 Methodology Output

This section presents and discusses performance parameters results obtained from the thermodynamic model such as indicated power (kW) with the indicated mean effective pressure (IMEP) and thermal efficiency (%) with specific fuel consumption (SEC, g/kW-hr) for determining at different computing condition such as engine speed, equivalence ratio and compression ratio, which were done using MATLAB program. The model needs lots of parameters which are distinguished such as engine geometries, fuel-air properties, and engine operating condition, in order to predict results. However, these were assumed in details of known parameters, mainly for the single cylinder four stroke spark ignition without turbo or super charger and exhaust gas recirculation (EGR) system engine while the model was developed under no-load operating condition. The pre-mixer model of intake manifold were computed by using multi-fuel and were compared with the old numerical carburetor Sendyka[10] (indirect injection) and fuel injector (direct injection) by Ferguson [8]. An assumption on engine specification to be used in the calculation is shown in Table 1 as below.

Table 1 The specifications for Calculation [4 and 5]

Input parameters	Values
Bore, (m) /Stroke (m)	0.068/0.045
Stroke/2(rod Length)	0.25
Fuel(Gasoline (G), Ethanol(E))	%Vol, G90E10 (LHV [4 and 5])
Start of pressure/tem (kPa)/(K)	100/350
Start of intake process	-360 crank angle
Start of compress process	-180 crank angle
Start of combustion process	-20 BTDC crank angle
Finish of combustion process	40 ATDC crank angle
Finish of expansion process	180 crank angle
Finish of exhaust process	360 crank angle
Fuel inject/Carburetor model	[10, 8]
Computing condition	**(Output) Axis X**
Equivalence ratio	0.8 to 1.2
Compression ratio	8 to 12
Engine speed	1000 to 3000
Engine performances	**(Output) Axis Y**
Thermal efficiency with SFC	Pre-mixer,Carburetor[10],Fuel injector[8]
Indicated Power with IMEP	Pre-mixer,Carburetor[10],Fuel injector[8]

4.2 Effects of engine speed for the engine performances

The effect of engine speed for power (kW) and mean pressure (bar) are presented in Figure 3, The graph shows the indicted power and indicated mean effective pressure for the engine speed, the carburetor, the injector and the pre-mixer have similar levels, with the high start point and the steadily falling to low point, according to the performance of engine and the engine speed of internal combustion engine. All intake manifold system processes of indicated mean effective pressure have opposite line trends with the low start point and then slightly rising. In contrast, the changed value above lines from this numerical computed engine is caused by the indicated power depended on the peak pressure in the combustion stroke, but indicated mean effective pressure depends on all of engine cycle and this numerical engine fix the constant friction. These results of indicated power must be decreased the trend lines if the numerical calculate at 4,000 rpm and indicated mean effective pressure must increase the trend lines at the same engine speed.

The effect of engine speed for combustion and wasted fuel is presented in Figure 4. The percentage of thermal efficiency (%) of the carburetor and pre-mixer show the same data value with engine speed, and this thermal efficiency of the intake system showed the same graph trends. The specific fuel consumption (SEC, g/kW-hr) of injector and pre-mixer show the same trends value with low start and then rise to the highest engine speed point of 3,000 . In addition, the carburetor and pre-mixer overlap in this graph.

The higher value of thermal efficiency is the injector system and these trend line results of thermal efficiency may be constant if the numerical calculation is at 4,000 rpm. The higher value of specific fuel consumption is the carburetor or pre-mixer and may be increasing if the engine speed is computed more than this condition.

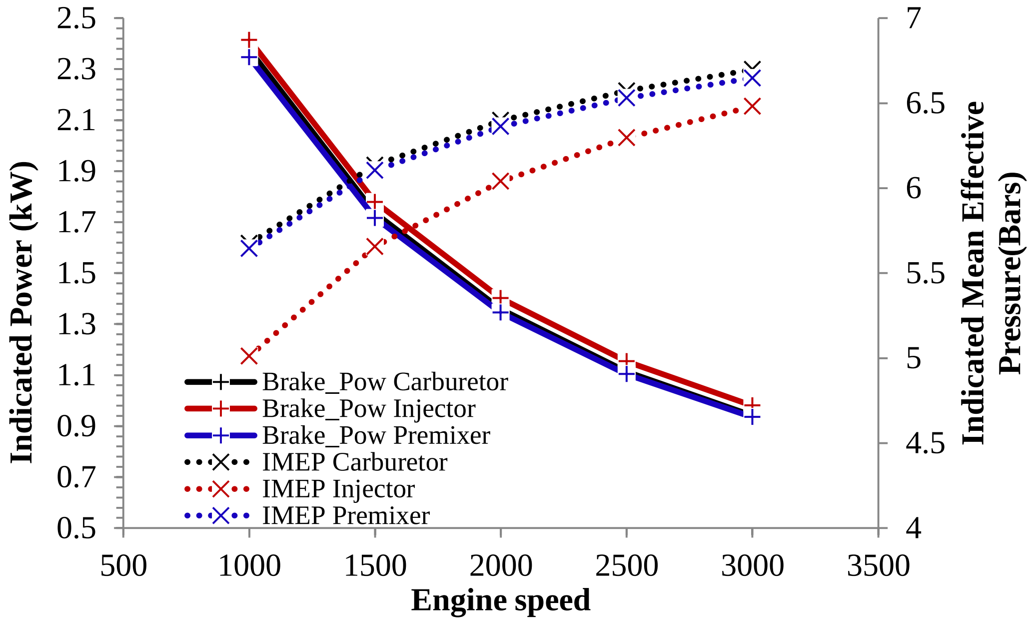

Figure 3 : The effect of engine speed for Carburetor, Injector and Pre-mixer on Indicated Power and Indicated Mean Effective Pressure

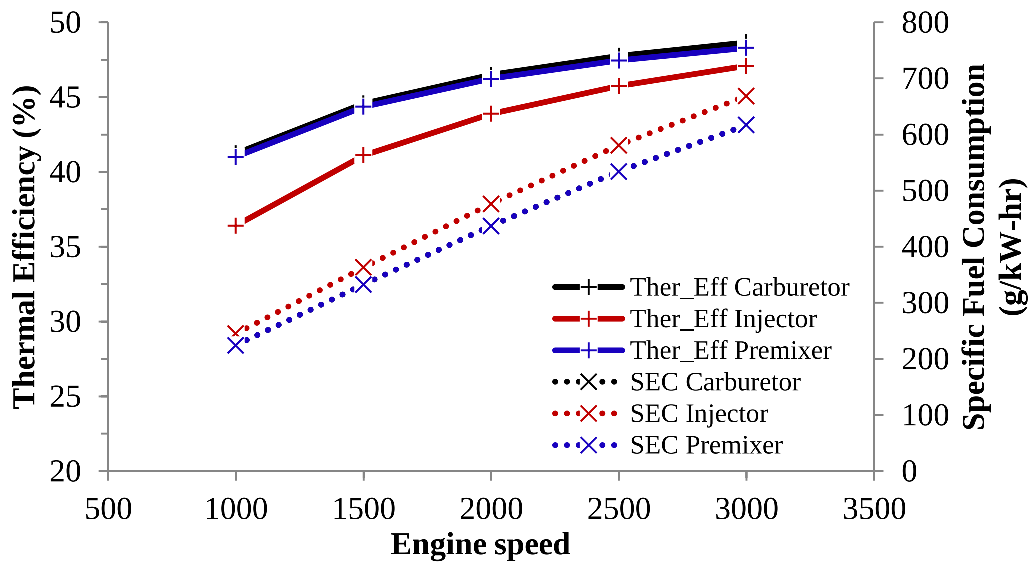

Figure 4 : The effect of engine speed for Carburetor, Injector and Pre-mixer on Indicted Thermal Efficiency and Specific Fuel Consumption

4.3 Effects of equivalence ratio for the engine performances

The effect of equivalence ratio for power (kW) and pressure (bar) are presented in Figure 5. These results show the indicated power of the carburetor and the pre-mixer shows the similar levels rising slightly with the equivalence ratio of 0.8 to 1.2 while the injector has risen after it has remained stable for 1.0 to 1.2 equivalence ratio.

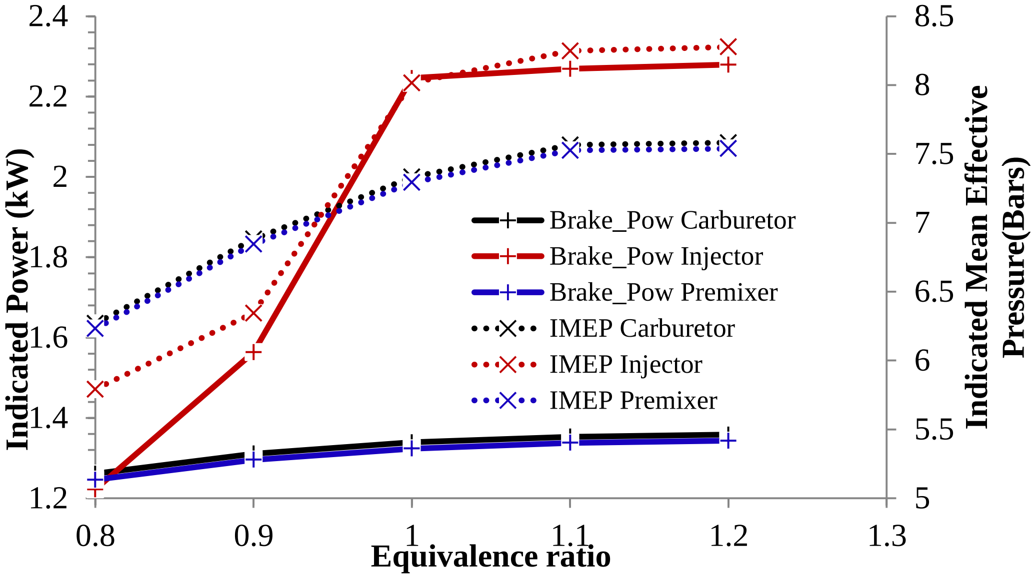

Figure 5 : The effect of equivalence ratio for Carburetor, Injector and Pre-mixer on Indicated Power and Indicated Mean Effective Pressure

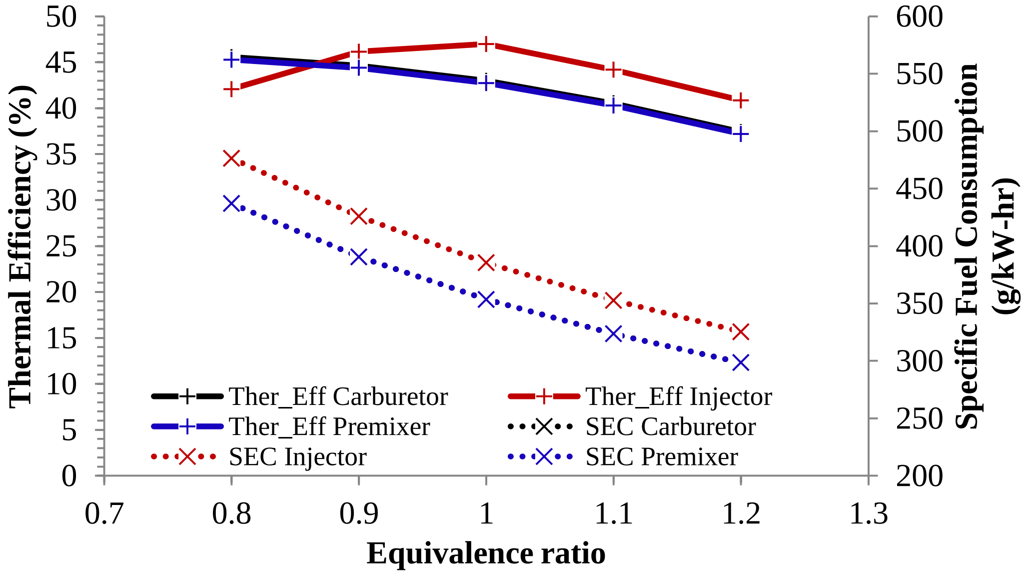

Figure 6 : The effect of equivalence ratio for Carburetor, Injector and Pre-mixer on Indicted Thermal Efficiency and Specific Fuel Consumption

The indicated mean effective pressure for three intake manifold system processes showed as the same trends with the indicated power. The increasing of indicated power is due to the increasing rate in equivalence ratio of fuel , and the higher energy is expectedly observed by exothermic energy. But if the equivalence ratio more than 1, this process means the decreasing oxygen for combustion, according to exothermic energy is the lowest value with the low equivalence ratio. The changing of carburetor and pre-mixer has a few values throughout the increasing equivalence ratio. But the fuel injection system is the significant change more than other intake systems.

The effect of equivalence ratio for combustion and wasted fuel are presented in Figure 6. The graph provides the percentage of thermal efficiency (%) and specific fuel consumption (SEC, g/kW-hr) trends of three intake manifold system processes with equivalence ratio. Thermal efficiency for carburetor and pre-mixer showed the same trends and has the lowest when comparing with fuel injection. Specific fuel consumption of injector and pre-mixer (or carburetor is due to almost the same value) show the same trends and not different value, the injector and pre-mixer starts high and then drop to its lowest point 1.2 of equivalence ratio. These results mean that the lowest equivalence ratio have the higher oxygen than equivalence ratio 1.0 to 1.2, according to the complete combustion. In the effect of intake system, the fuel injection significantly changes more than other intake systems.

4.4 Effects of compression ratio for the engine performances

The effect of compression ratio for power (kW) and pressure (bar) are presented in Figure 7, The three intake manifold system processes of indicated power and indicated mean effective pressure showed the similar steadily fall trends from the high point start to low point throughout the compression ratio 8 to 9 range. These results showed the effect of volume in cylinder engine according to the power and average pressure in this system.

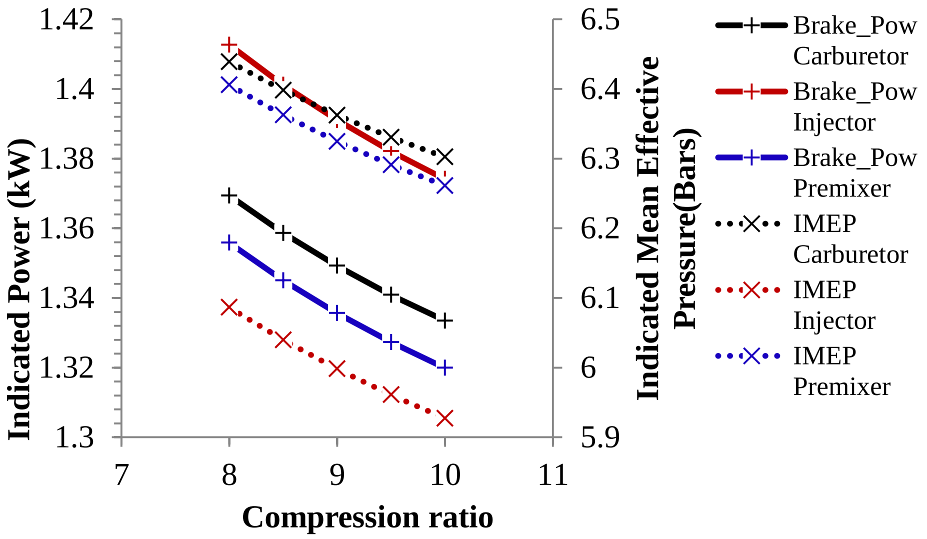

Figure 7 : The effect of compression ratios for Carburetor, Injector and Pre-mixer on Indicated Power and Indicated Mean Effective Pressure

The effect of compression ratio for combustion and wasted fuel are presented in Figure 8, the injector showed the lowest thermal efficiency and the remaining stable throughout the compression ratio. The carburetor and pre-mixer systems showed the same rising sharp trends from 8 to 10 compression ratios with the carburetor gave the highest thermal efficiency. All three intake manifold system processes showed the same trends of specific fuel consumption (SEC, g/kW-hr) with the compression ratio which the pre-mixer and carburetor showed the same value (blue line). This is due to the increasing compression ratio is not affect the rate of mass fuel and air into cylinder and in this numerically computed engine by constant value.

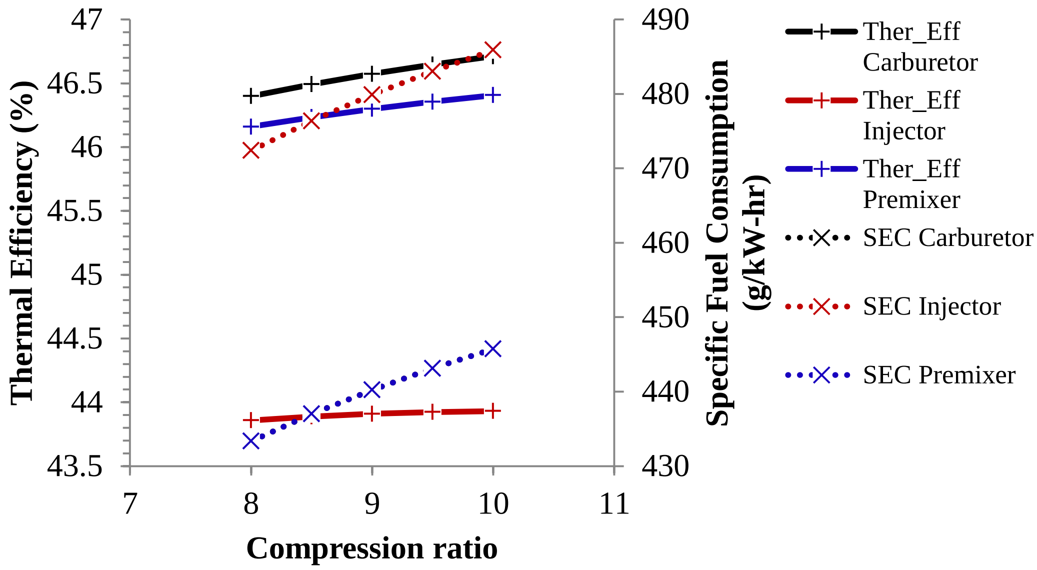

Figure 8 : The effect of compression ratio for Carburetor, Injector and Pre-mixer on Indicted Thermal Efficiency and Specific Fuel Consumption

5 Conclusions and Suggestions

5.1 Conclusions

Effect of engine speed, the indicated power and indicated mean effective pressure for the engine speed variations, the carburetor and pre-mixer had similar levels with are overlap line trend values, but fuel injector seem the highs value about 10% for all values and significantly changes, therefore these are according to the performance of engine and following to the engine speed of internal combustion engine. All intake manifold systems have results no difference of this computed by the condition. The thermal efficiency of the carburetor and pre-mixer show the same data value with engine speed but have the lowest vale when compared with fuel injection system, the difference value are 5 % from this intake system. The specific fuel consumption of injector and pre-mixer showed, these are the overlap trend lines a data in this graph. The higher value of thermal efficiency is the injector system. So, the effect of engine speed is not affecting the system changes significantly of pre-mixer and carburetor, except the fuel injector. The results obtained with presented theoretical model are in acceptable agreement with those other intake system. An agreement of 10% was determined between the pre-mixer and other intake system results

Effect of equivalence ratio, the indicated power and indicated mean effective pressure for the equivalence ratio variations, these results are the carburetor and the pre-mixer showed similar levels rising slightly with the equivalence ratio while the injector has risen obvious significantly changes and different value about 50%. In thermal efficiency for carburetor and pre-mixer are the same trends and has the lowest. Specific fuel consumption of injector and pre-mixer (or carburetor is due to the value almost the same) showed the same trends and not different value. In the effect of intake system, the fuel injection has significantly changes over more than other intake system. So, the effect of equivalence ratio is affecting the system changes significantly of pre-mixer with carburetor and fuel injector in the thermal efficiency. The results obtained with presented theoretical model are in acceptable agreement with those other intake system. An agreement of 50% was determined between the pre-mixer and fuel injector results

The effect of compression ratio, the indicated power and indicated mean effective pressure showed the similar steadily fall trends, the intake manifold system is significantly changes of the these performance parameters because different value about 5-10%. These results showed the effect of volume in cylinder engine according to the power and average pressure in this system as following theory. In thermal efficiency, fuel injector showed the lowest thermal efficiency and the remaining stable throughout the compression ratio. The carburetor and pre-mixer systems showed the same rising sharp trends of all compression ratios with the carburetor gave the highest thermal efficiency about 5-10 %. So this condition of compression ratio has significantly changes over more than other condition of computing. So, the effect of compression ratio is affecting the system changes significantly of pre-mixer with carburetor and fuel injector for the all of engine performances. The results obtained with presented theoretical model are in acceptable agreement with those other intake system. An agreement of 5 % was determined between the pre-mixer and fuel injector results

5.2 Suggestions and Future research.

Numerical engines are susceptible to changes and are therefore influenced by any changes. Further research could be done to determine the numerical influence of pulsating flow on the following:

- Effect of thee length and diameter for pre-mixer which connects cylinder engine.
- Effect of two phases (liquid fuel) by numerical investigation.
- Experiment investigation with pre-mixer, old carburetor and modified fuel injection which Single gasoline fuel
- Experiment investigation with pre-mixer, old carburetor and modified fuel injection which Multi fuel.

Acknowledgements
This research was supported by Energy Management Systems and Monitoring & Verification Control, Research & Development Center [ES-MVC]. Science and Technology Research Institute (STRI). King Mongkut's University of Technology North Bangkok.

References

[1] R. Yapici and K. Ersoy, Performance characteristics of the ejector refrigeration system based on the constant area ejector flow model, *Energy Conversion and Management 46*, p. 3117–3135, (2005).

[2] R.Z. Wang, S. He and Y. Li, "Progress of mathematical modeling on ejectors, *Renewable and Sustainable Energy Reviews Volume 13, Issue 8,* , p 1760–1780, (2009).

[3] L. Chaqing, Gas ejector modeling for design and analysis. Ph.D thesis, Texas A&M University, 2008.

[4] S. Thanakom, The Final report, "Study on the Small Size Single Cylinder Gasoline and Diesel Engines, Draft of Ministerial Regulation on specification on Energy Efficiency with the Energy Conservation Promotion Act (No.2) B.E. 2550 (2007)", Department of Alternative Energy Development and Efficiency (DEDE), Ministry of Energy. (2001).

[5] J. Paramust and S. Thanakom, The Thermodynamic model of a Small Size Single Cylinder Four Stroke Spark Ignition Engine using Gasoline RON 91 Thailand Fuel and Comparisons with Experiment. Proceeding of The 8th International Conference on Automotive Engineering, (2012).

[6] D. R. Buttsworth, Spark Ignition Internal Combustion Engine Modeling using Matlab, Faculty of Engineering & Surveying Technical Reports, University of Southern Queensland, 2002.

[7] S. Ramachandran, Rapid Thermodynamic Simulation Model of an Internal Combustion Engine on Alternate Fuels. Proceedings of the International MultiConference of Engineers and Computer Scientists 2009 Vol III, 2009.

[8] C. R. Ferguson, Internal Combustion Engines, Applied Thermosciences. New York: John Wiley and Sons, 1986.

[9] G. H. Abd Alla, Computer simulation of a four stroke spark ignition engine. *En. Convers. Mng., vol. 43,* p. 1043-1061. (2002).

[10] B. Sendyka and J. Filipczyk., Simulation of the Characteristic of a Carburetor of an Internal Combustion Engine. *SAE Technical Paper 1995-02-019 50987*, (1995).

[11] R. B. Krieger and G. L. Borman., The Computation of Apparent Heat Release for Internal Combustion Engines. *America Society of Mechanical Engineering*, 66-WA/DGP-4. 1966.

Received: April 23, 2014